

Gas Sensing for Commercial Refrigerants R-134a and R-1234yf Using Rotational Absorption Spectroscopy in the 220–330 GHz Frequency Range

M. Arshad Zahangir Chowdhury¹ · Timothy E. Rice¹ · Megan N. Powers¹ · Muhammad Waleed Mansha² · Ingrid Wilke³ · Mona M. Hella² · Matthew A. Oehlschlaeger¹

Received: 6 October 2021 / Accepted: 29 August 2022 / Published online: 6 September 2022 © The Author(s), under exclusive licence to Springer Science+Business Media, LLC, part of Springer Nature 2022

Abstract

The detection of gaseous refrigerants, necessary for industrial control and environmental monitoring, is explored using rotational spectroscopy in the THz wave region. Rotational absorption spectra for two widely used commercial hydrofluorocarbon (HFC) refrigerants, 1,1,1,2-tetrafluoroethane (R-134a or HFC-134a) and 2,3,3,3-tetrafluoropropene (R-1234yf or HFO-1234yf), are characterized in the 220-330 GHz frequency range at room temperature (297 K) and modest pressures (0.25-8 Torr) using a compact microelectronics-based THz wave spectrometer. The absorption spectra illustrate complex, broad, and repeating structures that result from the blending of hundreds of pressure-broadened rotational lines. The unique and distinct spectra for R-134a illustrate potential for its detection in the present frequency region with estimated detection limits approaching 15 ppm per meter path length in 1 atm of air. The spectra for R-1234yf are less distinct than those for R-134a and illustrate complex structured rotational absorption features in combination with an underlying quasi-continuous absorption that increases in strength to higher frequencies. To our knowledge, this is the first experimental characterization for the spectra of R-134a and R-1234yf in this frequency region.

Keywords R-134a \cdot R-1234yf \cdot Refrigerants \cdot Gas sensing \cdot Rotational spectroscopy \cdot Terahertz \cdot THz wave

M. Arshad Zahangir Chowdhury chowdm@rpi.edu

Department of Mechanical, Aerospace, and Nuclear Engineering, Rensselaer Polytechnic Institute, Troy, USA

Department of Electrical, Computer, and Systems Engineering, Rensselaer Polytechnic Institute, Trov. USA

Department of Physics, Applied Physics, and Astronomy, Rensselaer Polytechnic Institute, Troy, USA

1 Introduction

Hydrofluorocarbons (HFCs) are replacing hydrochlorofluorocarbons (HCFCs) and chlorofluorocarbons (CFCs) as commercial refrigerants, owing to their reduced global warming potential and decreased impact on stratospheric ozone [1]. To reduce the deleterious impact of refrigerants on the ozone layer, the Montreal Protocol established the elimination of CFC production by 2010 and elimination of HCFC production by 2030 [2]. Today, widely used commercial HFC refrigerants include 1,1,1,2-tetrafluoroethane (R-134a or HFC-134a) and 2,3,3,3-tetrafluoropropene (R-1234yf or HFO-1234yf). Gas sensors for these refrigerants are desired such that their release to the atmosphere can be monitored, controlled, and mitigated in industrial settings during their manufacture, use, and destruction.

R-134a is currently the most commonly used refrigerant in automotive air conditioning systems and in-home and commercial chillers and refrigeration [3]. It was introduced in the 1990s as a replacement for the HCFCs R-12 (dichlorodifluoromethane) and R-22 (chlorodifluoromethane), in part due to its lower global warming potential (GWP) [1]. The GWP is a relative measure of the heat absorbed by one-unit mass of a greenhouse gas over a 100-year time period, relative to the heat absorbed by one-unit mass of CO₂. Hence, the GWP for CO₂ is 1. The 100-year GWP for R-134a is 1430 and is somewhat lower than the 100-year GWP for R-12 and R-22 which are 2400 and 1810, respectively [1]. While R-134a has lower GWP than its HCFC predecessors, R-134a is still a strong greenhouse gas and is on the Intergovernmental Panel on Climate Change (IPCC) list of greenhouse gases [4, 5].

R-1234yf, a hydrofluoroolefin (HFO), has been developed as a replacement for R-134a and has a 100-year GWP of less than 1, more than a thousand times lower than of R-134a [6, 7]. R-1234yf is currently undergoing wide acceptance to meet increasingly stringent government regulations on greenhouse gases, including a 2015 European Union regulation that restricts the use of HFCs by 2030 to below 79% of the 1990 levels and imposes stricter standards for testing, monitoring, and handling refrigerants [6]. HFOs, including R-1234yf, are mildly flammable, are asphyxiants at high concentrations, and are odorless. Hence, their use poses dangers and requires monitoring and control of their release.

Spectroscopy-based gas sensing for refrigerants has not been widely investigated in the literature and the studies that do exist have mostly considered infrared frequencies where vibrational transitions exist (e.g., [8]). There have been some fundamental studies of rotational spectroscopy for refrigerants, carried out in the farinfrared, THz, millimeter wave, or microwave regions, including those carried out for legacy refrigerants R-11 (trichlorofluoromethane, CCl₃F) and R-22 (chlorodifluoromethane, CHClF₂) quantifying transition frequencies, strengths, and in some cases collisional broadening [9, 10, 11, 12]. Similar fundamental rotational spectroscopy studies have been carried out for the HFC refrigerant R-32 (difluoromethane, CH₂F₂) [13, 14, 15, 16]. Less information is available in the literature for R-134a and R-1234yf, apart from prior high-resolution infrared measurements in which rotational constants and distortion parameters have been reported [17, 18]. Ogata and Miki [19] have characterized the microwave absorption of R-134a in a region

from 8 to 26 GHz. The rotational spectrum of R-134a was studied again using FTIR, Raman, and microwave measurements by Xu et al. [20], in which they determined the rotational constants. Wong et al. [21] have examined a portion of far-infrared spectrum of R-134a, characterizing vibrationally excited states and confirming the rotational constants reported by Xu et al. [20]. Cazzoli et al. [22] have measured collisional linewidths for three R-134a transitions at frequencies around 84 and 105 GHz, for self-broadening and broadening by N₂ and O₂. For R-1234yf, Marshall et al. [23] have characterized the rotational spectrum in the microwave region from 6 to 18 GHz and reported rotational constants. To our knowledge, no studies exist for R-134a or R-1234yf close to the frequency range considered in the current study.

Sensors exist in large commercial refrigeration and air conditioning systems, but in most cases do not seek to directly detect refrigerant leaks. Instead, they rely on temperature measurements, where changes in temperature or unexpected temperature measurements may indicate the presence of a leak [24]. Refrigerant gas sensors, based on THz wave spectroscopy, may provide leak detection in industrial processes involving refrigerants, including their production, use, and destruction. Microelectronic THz wave sensing can provide quantitative gas sensing that is non-intrusive, selective, sensitive, and robust against particle/aerosol interference and water vapor. Ultimately, such sensors, based on silicon microelectronic fabrication processes, could also be inexpensive and automated using machine learning—based sensing methods [25]. Here we characterize the absorption spectra for R-134a and R-1234yf in the 220–330 GHz region and explore the potential for an electronic THz wave gas sensor for these two refrigerants.

2 Experimental Methods

Our group has recently reported THz wave gas sensing for VOCs [26] and halogenated hydrocarbons [27] using rotational absorption in the 220–330 GHz range based on an electronic THz wave source. In the present work, the same experimental setup and procedures were used as in the prior work by Rice et al. [26, 27] and Mansha et al. [28, 29]. THz wave radiation (220–330 GHz) is generated via an electronic source that involves the frequency multiplication of a radio frequency signal. The THz wave radiation is collimated with a Teflon lens, passed through a HDPE gas cell with 45° angled windows containing the gaseous refrigerant of interest (path length of 21.59 cm), and focused onto a Schottky diode detector with a second Teflon lens. To increase the signal-to-noise, the THz wave signal is amplitude modulated and the signal detected on the Schottky diode is demodulated using a lock-in amplifier to extract a DC signal proportional to the radiation intensity. In a given experiment, the THz wave frequency is swept from 220 to 330 GHz, while amplitude modulated, to measure an absorption spectrum. See Fig. 1 for a schematic of the experimental setup.

The Beer-Lambert law is used to determine the absorbance A, based on the transmitted THz wave signal (I) and the reference signal (I_0), measured while the gas cell is under vacuum:

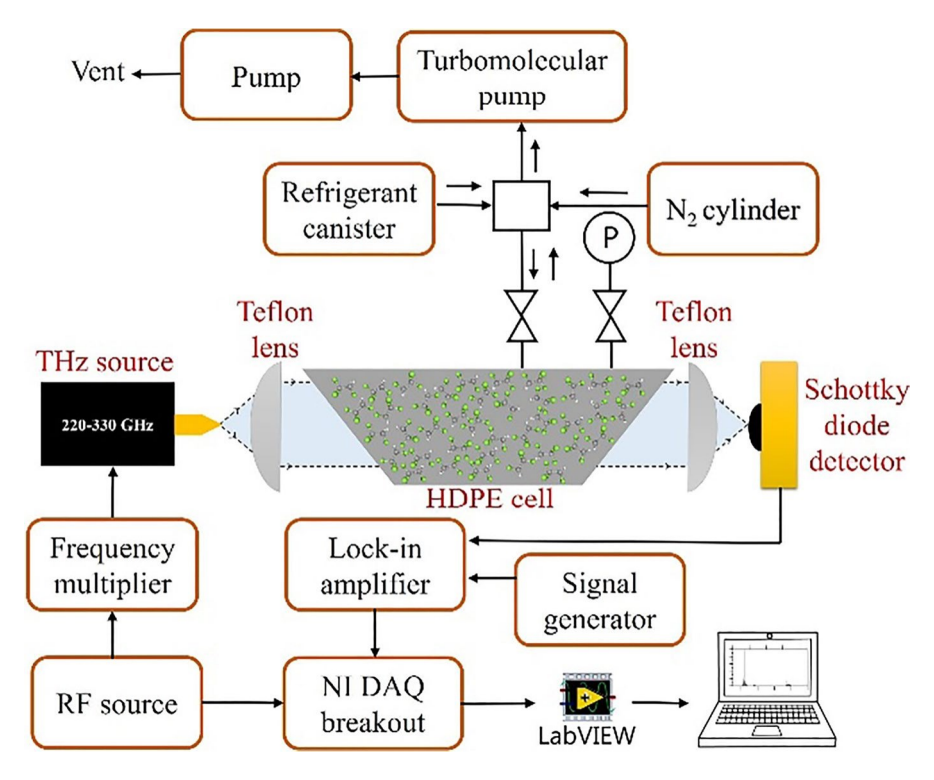


Fig. 1 Schematic diagram of experimental setup

$$-In(I/I_0) = (P, T, c)cL = A$$

where ε (v, P, T, c) is the absorption coefficient, c is the molar concentration of the absorbing gas, and L the optical path length. The absorption coefficient depends on frequency v, thermodynamic conditions (pressure P and temperature T), and gas sample concentrations (through collisional line broadening contributions). See Fig. 2 for an example measurement of the transmitted and reference signals and the resulting absorption spectrum.

3 Results and Discussion

Spectral absorption measurements were made in the 220–330 GHz range for pure R-134a and R-1234yf at 297 K and at the pressures listed in Table 1. Refrigerants were sourced from Honeywell. The rotational constants from the literature [20, 23] for both refrigerants are listed in Table 1.

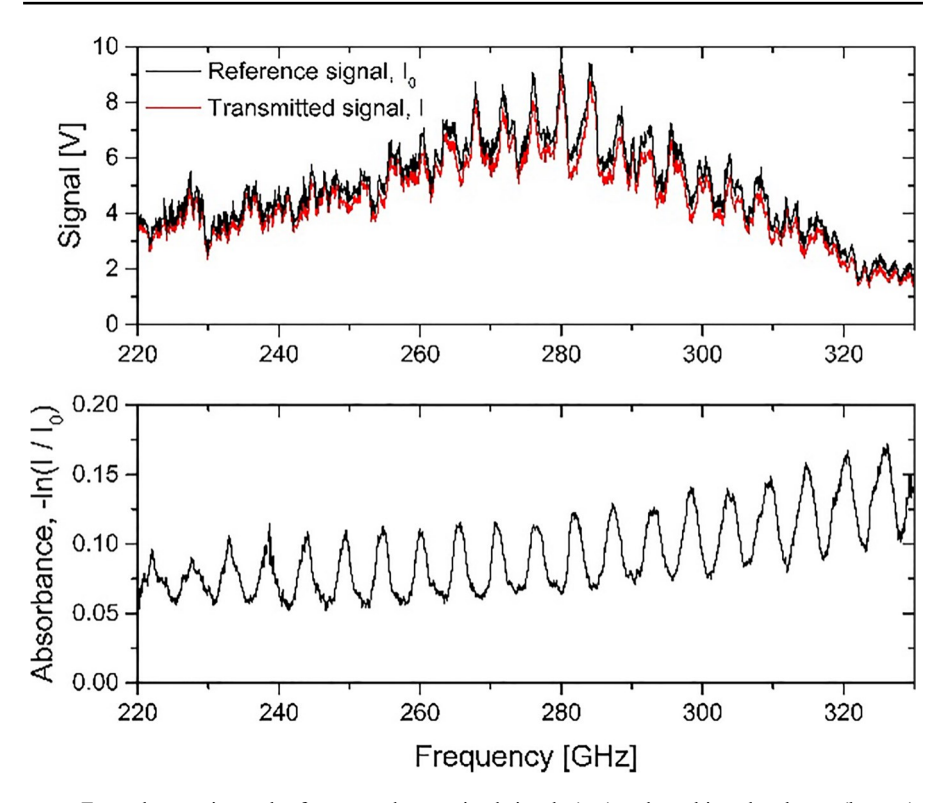


Fig. 2 Example experimental reference and transmitted signals (top) and resulting absorbance (bottom); conditions: R-134a at 8 Torr and 297 K

Table 1 Experimental conditions and rotational constants for the refrigerants considered

Refrigerant	Experimental pressures [Torr]	Rotational constants
R-134a (1,1,1,2-tetra- fluoroethane, CH ₂ FCF)	1.5, 2, 4, 8	$\begin{array}{l} A = 5355.61817 \ \text{MHz} \\ B = 2799.22085 \ \text{MHz} \\ C = 2759.43294 \ \text{MHz} \\ \delta_J = 0 \\ \delta_K = 1.766 \ \text{kHz} \\ \Delta_J = 0.5012 \ \text{kHz} \\ \Delta_{JK} = 4.3132 \ \text{kHz} \\ \Delta_{K} = -3.396 \ \text{kHz} \\ \text{Source: Xu et al. [20]} \end{array}$
R-1234yf (2,3,3,3-tetra-fluoropropene, CH ₂ =CFCF ₃)	1.5, 2, 4	$\begin{array}{l} A = 3714.71903 \ \ MHz \\ B = 2465.51465 \ \ MHz \\ C = 2001.09445 \ \ MHz \\ \delta_J = 0.05784 \ \ kHz \\ \delta_K = -2.5308 \ \ kHz \\ \Delta_J = 0.2570 \ \ kHz \\ \Delta_{JK} = 1.0862 \ \ kHz \\ \Delta_{JK} = -0.8494 \ \ kHz \\ Source: Marshall et al. [23] \end{array}$

3.1 R-134a

Measured spectra for pure R-134a are shown in Fig. 3. These are, to our knowledge, the first such measurements for R-134a in the current frequency range. R-134a is a near-prolate asymmetric top and its rotational spectra in the Fig. 3 frequency range contain strong repeating features, resulting from the blending of pressure-broadened transitions. These repeating features are spaced at frequencies of approximately $B+C=\sim 5.6$ GHz, indicating that these repeating structures arise from strong R-branch a-type transitions, common in near-prolate polar molecules. The selection rules for R-branch a-type transitions are $\Delta J=+1$, $\Delta K_a=0$, and $\Delta K_c=+1$, where J is the quantum number for total rotational angular momentum and K_a and K_c are the quantum numbers for the projection of total angular momentum onto the a- and c-axes. The repeating R-branch a-type structures, centered at frequencies of (B+C)(J''+1), sit on top of a continuum absorption, or baseline, that is likely formed by the blending of the hundreds of weaker pressure-broadened transitions in this frequency range.

Spectral simulations for R-134a were carried out using the PGopher code [30], which provides assignment of transitions based on the rotational constants (Table 1) with relative line intensities based on the thermal population distribution function.

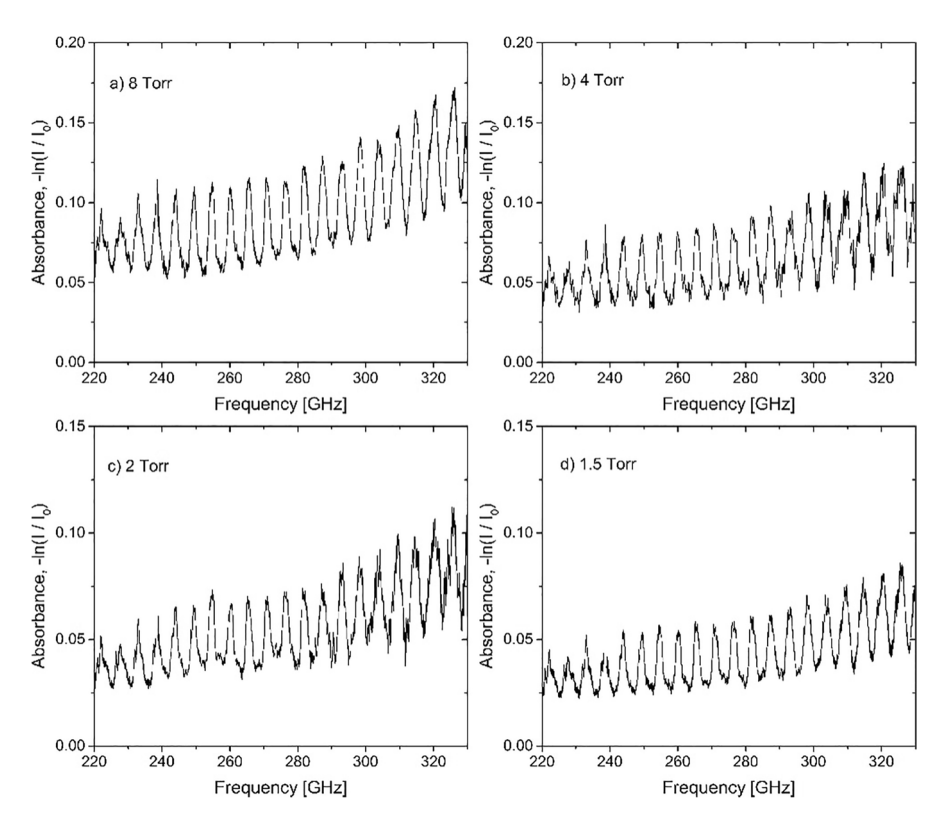


Fig. 3 Measured absorption spectra for R-134a at 297 K for a 8 Torr, b 4 Torr, c 2 Torr, and d 1.5 Torr

See Fig. 4 (bottom panels) and Fig. 5 for transition frequencies for R-134a. All predicted strong transitions are R-branch a-type ($\Delta J = +1$, $\Delta K_a = 0$, and $\Delta K_c = +1$) and are clustered into bands belonging to common lower-state total rotational quantum numbers J''. For the current frequency range, twenty overall features are observed for $J' = 40 \leftarrow J'' = 39$ to $J' = 60 \leftarrow J'' = 59$, where J' is the upper-state total rotational quantum number. As shown in Fig. 5, within each band (common J''), all strong transitions have $\Delta K_a = 0$ and $\Delta K_c = +1$, where the strength of each transition is controlled by the population in the lower state at 297 K, governed by the lower-state energy.

Line broadening is also simulated to generate spectra that could be qualitatively compared to the current measurements, as shown in Fig. 4 (top two panels). A collisional linewidth of 29 MHz/Torr is used in these simulations, as measured by Cazzoli et al. [22] for R-134a rotational transitions at lower frequencies (\sim 84 and \sim 105 GHz for transitions emanating from J''=9, 14, and 19). The simulated pressure-broadened spectra agree qualitatively with the measurements, as they capture the frequencies of peak absorption and the spectral shape. However, the simulations do not capture the continuum background absorption that is observed

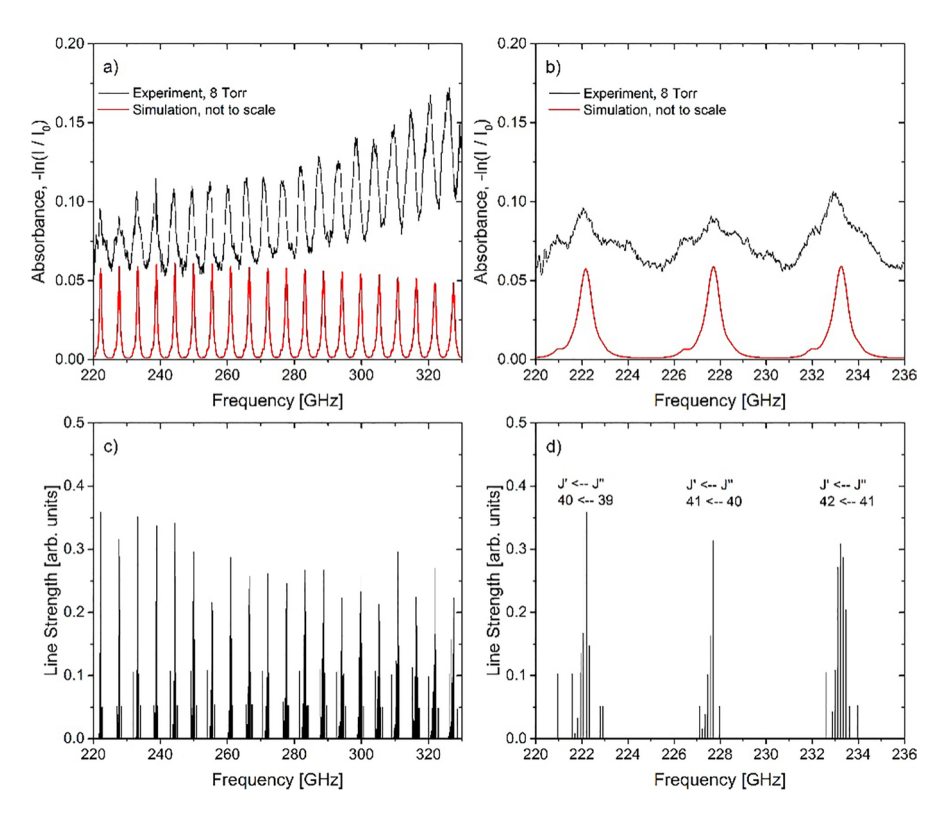
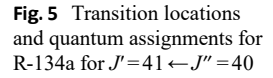
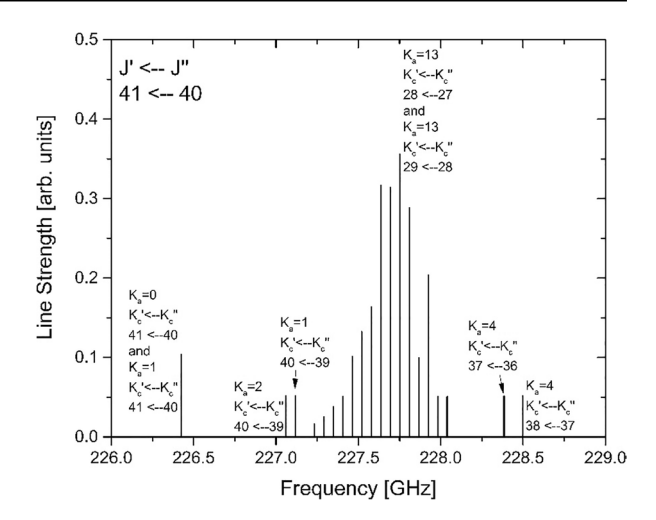


Fig. 4 Simulated and experimental spectra for R-134a and transition locations. **a, b** Experiment at 8 Torr and 297 K compared with simulation (not to scale) in two different frequency ranges. **c, d** Simulated line strengths in two different frequency ranges





experimentally. This is likely due to the fact that hundreds of weaker transitions are not considered in the simulation; e.g., Q-branch transitions are truncated from this simulation due to their low intensity.

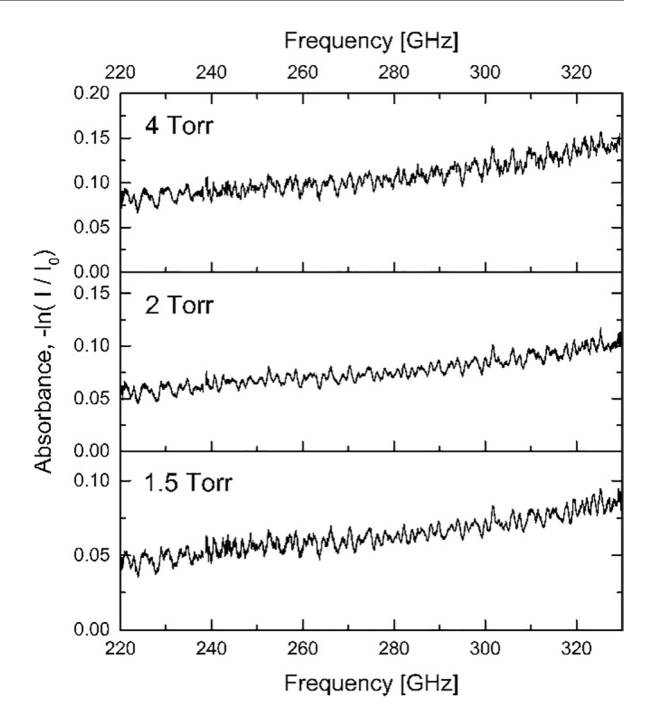
Note, there are no prior line strength measurements for R-134a in the current frequency region and, therefore, it is not possible to quantitatively compare simulated and measured spectra. Hence, the simulated absorbance values in Fig. 4 are not to scale. In any case, the spectral simulations are in qualitative agreement with the current measurements, which provide new information regarding the continuum background absorption and motivate future line strength measurements for R-134a in this frequency region.

Given the distinct and repeating nature of the for R-134a spectra, the current frequency range offers potential for sensing R-134a with an electronic THz wave absorption sensor, such as implemented in the current study. Certainly, under low-pressure conditions, with minimal pressure-broadening, R-134a can be detected at relatively low concentrations. Based on the measured absorption for pure R-134a at a path length of 21.59 cm (Fig. 3), and assuming a minimum detectable absorbance of 10^{-4} , which is achievable in a spectrometer with spectral or temporal averaging, we estimate a minimum detectable pressure of ~ 0.6 mTorr or $\sim 2 \times 10^{13}$ molecules/cm³ per meter of absorption path length. For the determination of the detection limits for trace quantities of R-134a in air at atmospheric pressure, we assume pressure-broadening parameters reported by Cazzoli et al. [22] for N₂ and O₂ as collision partners, resulting in an estimated minimum detectivity of ~ 15 ppm of R-134a in air per meter of absorption path length.

3.2 R-1234yf

Measured spectra for pure R-1234yf are shown in Fig. 6. To our knowledge, this is the first absorption measurement reported for R-1234yf in this frequency range. The spectra illustrate repeating structures that are less distinct than for R-134a and sit on a continuum background absorption that increases in strength

Fig. 6 Measured absorption spectra for R-1234yf at 297 K and 4 Torr (top), 2 Torr (middle), and 1.5 Torr (bottom)



to higher frequencies. The spectroscopy of R-1234yf is similar but more complex than R-134a. Again, strong R-branch a-type transitions ($\Delta J = +1$, $\Delta K_a = 0$, and $\Delta K_c = +1$) result in the repeating structures that are spaced in frequency at approximately $B+C=\sim 4.5$ GHz. In the case of R-1234yf, these repeating structures blend into each other to a high degree, as transitions that occur for different K_c " (lower-state quantum number for projection of angular momentum onto c-axis) are spread out in frequency to a greater degree than for R-134a, due to the greater rotational asymmetry for R-1234yf.

Again, spectral simulations for R-1234yf were carried out using the PGopher code [30] with the rotational constants found in Table 1. Figure 7 shows transition frequencies for R-1234yf and spectral simulations. The spectral simulations assume the same broadening parameters as for R-134a. To our knowledge, no broadening parameters have been reported for R-1234yf.

As in the case of R-134a, all predicted strong transitions for R-1234yf are R-branch a-type transitions. In the current frequency range (220–330 GHz), a very large range of total rotational quantum number appear, from J''=45 to J''=82, and the transitions for particular $J' \leftarrow J''$ change are spread in frequency space to the order of tens of GHz. See the Fortrat diagram in the bottom right panel of Fig. 7. It illustrates the strongest transitions in the 220 to 236 GHz range occur for J''=45 to J''=57. These transitions occur for a large number of K_a and K_c combinations, from $K_a''=0$ to $K_a''=J''$ and for $\Delta K_c=+1$, resulting in the larger frequency spread of transitions for a common J'' and the blended, less distinct, spectra for R-1234yf.

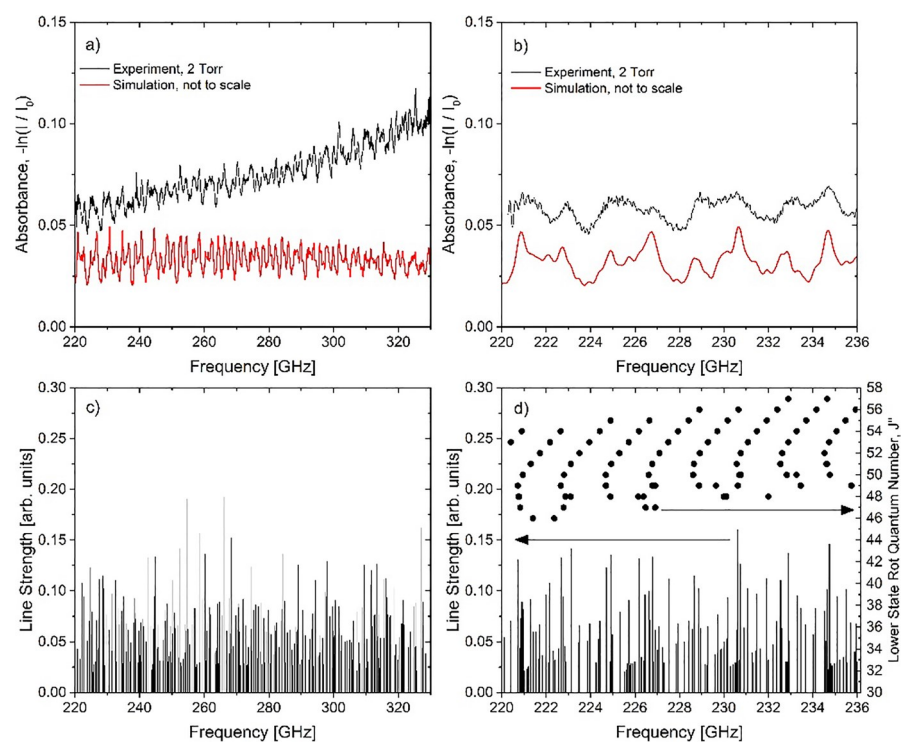


Fig. 7 Simulated and experimental spectra for R-1234yf and transition locations. a, b Experiment at 2 Torr and 297 K compared with simulation (not to scale) in two different frequency ranges. c, d Simulated line strengths in two different frequency ranges

The pressure-broadened spectral simulations illustrate loose qualitative agreement for the local shape of the spectra (top right panel of Fig. 7); i.e., they approximately capture the repeating nature of the spectra. As expected, the simulations do not capture the observed continuum absorption that increases in strength to higher frequencies, likely caused by weak rotational transitions (non R-branch a-type) that are not accounted for in the simulations. Again, the simulations are not intended to provide quantitative absorption and are not plotted to scale in Fig. 7.

Gas sensing for R-1234yf at dilute conditions in air in the current frequency range is less promising than for R-134a, due to the less distinct spectra for R-1234yf. However, measurements of R-1234yf under low-pressure conditions are certainly feasible, as demonstrated here. We estimate a minimum detection limit of $\sim 5 \times 10^{13}$ molecules/cm³ per meter of absorption path length for pure R-1234yf.

4 Conclusions

Rotational absorption spectroscopy measurements are reported for commercial refrigerants R-134a and R-1234yf at frequencies from 220 to 330 GHz for room temperature conditions (297 K) and modest pressures (1.5–8 Torr). Measurements

were carried out using an electronic THz wave spectrometer to characterize, for the first time, the absorption of these two refrigerants in the 220–330 GHz frequency range and to investigate the potential for THz wave gas sensing for these refrigerants. Measurements are compared with simulations of transition frequencies and pressure-broadened spectra. The measured spectra for R-134a demonstrate strong distinct repeating peaks, illustrating the potential for electronic THz wave gas sensors. We estimate a minimum detectivity of $\sim 2 \times 10^{13}$ molecules/cm³ per meter of absorption path length for pure R-134a and ~ 15 ppm per meter of absorption path length for R-134a dilute in air at atmospheric conditions. The spectra for R-1234yf are highly blended and illustrate spectroscopic complex-ity for this larger molecule having a higher degree of rotational asymmetry than R-134a. We estimate a minimum detectivity of $\sim 5 \times 10^{13}$ molecules/cm³ per meter of absorption path length for pure R-1234yf.

Funding This research was funded by the National Science Foundation under Grant CBET-1851291.

Data Availability The datasets generated and/or analyzed during the current study are available from the corresponding author on reasonable request.

References

- 1. J. M. Calm, P. Domanski, ASHRAE J. 46, 29-39 (2004).
- 2. C. Norman, S. DeCanio, L. Fan, Glob. Environ. Change 18, 330-340 (2008).
- A. Fortems-Cheiney, M. Saunois, I. Pison, F. Chevallier, P. Bousquet, C. Cressot, S.A. Montzka, P.J. Fraser, M.K. Vollmer, P.G. Simmonds, D. Young, J. Geophys. Res. Atmos. 120, 11-728 (2015).
- 4. R.K. Pachauri, M.R. Allen, V.R. Barros, J. Broome, W. Cramer, R. Christ, J.A. Church, L. Clarke, Q. Dahe, P. Dasgupta, N.K. Dubash, O. Edenhofer, I. Elgizouli, C.B. Field, P. Forster, P. Friedlingstein, J. Fuglestvedt, L. Gomez-Echeverri, S. Hallegatte, G. Hegerl, M. Howden, K. Jiang, B. Jimenez Cisneroz, V. Kattsov, H. Lee, K.J. Mach, J. Marotzke, M.D. Mastrandrea, L. Meyer, J. Minx, Y. Mulugetta, K. O'Brien, M. Oppenheimer, J.J. Pereira, R. Pichs-Madruga, G.K. Plattner, H.O. Pörtner, S.B. Power, B. Preston, N.H. Ravindranath, A. Reisinger, K. Riahi, M. Rusticucci, R. Scholes, K. Seyboth, Y. Sokona, R. Stavins, T.F. Stocker, P. Tschakert, D. van Vuuren, J.P. van Ypserle, Climate Change 2014: Synthesis Report. Contribution of Working Groups I, II and III to the Fifth Assessment Report of the Intergovernmental Panel on Climate Change, eds. R. Pachauri, L. Meyer (IPCC: Geneva, Switzerland, 2014).
- G.J. Velders, A.R. Ravishankara, M.K. Miller, M.J. Molina, J. Alcamo, J.S. Daniel, D.W. Fahey, S.A. Montzka, S. Reimann, Science 335, 922-923 (2012).
- 6. R. Ciconkov, Int. J. Refrig. 86, 441-448 (2018).
- 7. P. Arora, G. Seshadri, A.K. Tyagi, Cur. Sci. 115, 1497-1503 (2018).
- 8. A. Kosterev, G. Wysocki, Y. Bakhirkin, S. So, R. Lewicki, M. Fraser, F. Tittel, R.F. Curl, Appl. Phys. B 90, 165-176 (2008).
- 9. H.A.K.A.N. Altan, B.L. Yu, S.A. Alfano, R.R. Alfano, Chem. Phys. Lett. 427, 241-245 (2006).
- D.T. Cramb, Y. Bos, H.M. Jemson, M.C.L. Gerry, C.J. Marsden, J. Mol. Struct. 190, 387-400 (1988).
- 11. Z. Kisiel, L. Pszczolkowski, G. Cazzoli, G. Cotti, J. Mol. Spectrosc. 173, 477-487 (1995).
- Z. Kisiel, J.L. Alonso, S. Blanco, G. Cazzoli, J.M. Colmont, G. Cotti, G. Graner, J.C. Lopez, I. Merke, L. Pszczólstrok, J. Mol. Spectrosc. 184, 150-155 (1997).
- 13. L. Martinache, D. Boucher, J. Demaison, J.C. Deroche, J. Mol. Spectrosc. 119, 225-228 (1986).

- 14. N. Tasinato, G. Regini, P. Stoppa, A.P. Charmet, A. Gambi, J. Chem. Phys. 136, 214302 (2012).
- N. Tasinato, A. Turchetto, C. Puzzarini, P. Stoppa, A.P. Charmet, S. Giorgianni, Mol. Phys. 112, 2384-2396 (2014).
- N. Tasinato, G. Ceselin, A.P. Charmet, P. Stoppa, S. Giorgianni, J. Mol. Spectrosc. 348, 57-63 (2018).
- 17. C.D. Thompson, E.G. Robertson, C.J. Evans, D. McNaughton, J. Mol. Spectro. 218, 48-52 (2003).
- 18. J.J. Harrison, J. Quant. Spectro. Rad. Trans. 151, 210-215 (2015).
- 19. T. Ogata, Y. Miki, J. Mol. Struct. 140, 49-56 (1986).
- L.H. Xu, A.M. Andrews, R.R. Cavanagh, G.T. Fraser, K.K. Irikura, F.J. Lovas, J.U. Grabow, W. Stahl, M.K. Crawford, R.J. Smalley, J. Phys. Chem. A 101, 2288-2297 (1997).
- A. Wong, C. Medcraft, C.D. Thompson, E.G. Robertson, D. Appadoo, D. McNaughton, D. Chem. Phys. Lett. 634, 225-229 (2015).
- 22. G. Cazzoli, C. Puzzarini, L. Dore, J. Quant. Spectro. Rad. Trans. 83, 699-710 (2004).
- M.D. Marshall, H.O. Leung, B.Q. Scheetz, J.E. Thaler, J.S. Muenter, J. Mol. Spectrosc. 266, 37-42 (2011).
- 24. J.W. Yoo, S.B. Hong, M.S. Kim, Int. J. Refrig. 78, 157-165 (2017).
- 25. M.A.Z. Chowdhury, T.E. Rice, M.A. Oehlschlaeger, Appl. Phys. B. 127, 34 (2021).
- T.E. Rice, M.A.Z. Chowdhury, M.W. Mansha, M.M. Hella, I. Wilke, M.A. Oehlschlaeger, Appl. Phys. B 126, 1-12 (2020).
- T.E. Rice, M.A.Z. Chowdhury, M.W. Mansha, M.M. Hella, I. Wilke, M.A. Oehlschlaeger, Appl. Phys. B 127, 1-9 (2021).
- M.W. Mansha, K. Wu, T.E. Rice, M.A. Oehlschlaeger, M.M. Hella, I. Wilke, IEEE Sensors (2019), https://doi.org/10.1109/SENSORS43011.2019.8956555.
- M.W. Mansha, T.E. Rice, M.A. Oehlschlaeger, I. Wilke, M. M. Hella, IEEE Sensors J. 21, 4553-4562 (2021), https://doi.org/10.1109/JSEN.2020.3031838
- 30. C.M. Western, B.E. Billinghurst, Phys. Chem. Chem. Phys. 21, 13986-13999 (2019).

Publisher's Note Springer Nature remains neutral with regard to jurisdictional claims in published maps and institutional afiliations.

Springer Nature or its licensor holds exclusive rights to this article under a publishing agreement with the author(s) or other rightsholder(s); author self-archiving of the accepted manuscript version of this article is solely governed by the terms of such publishing agreement and applicable law.